UNIL | Université de Lausanne

LREN
Laboratoire de Recherche en Neuro-Imagerie

Early detection of idiopathic Parkinson's disease based on magnetic resonance imaging

Master project

2010-2012

Student
Khadidja Benkortbi

Tutor
Prof. Bogdan Draganski

LREN, Department of Clinical Neurosciences, CHUV

Experts
Dresse. Meritxell Bach-Cuadra, M.E.R.

CIBM, Center for Biomedical Imaging, CHUV/UNIL

TABLE OF CONTENTS:

ABSTRACT:

The diagnosis of idiopathic Parkinson's disease (IPD) is entirely clinical. The fact that neuronal damage begins 5-10 years before occurrence of sub-clinical signs, underlines the importance of preclinical diagnosis.

A new approach for in-vivo pathophysiological assessment of IPD-related neurodegeneration was implemented based on recently developed neuroimaging methods. It is based on non-invasive magnetic resonance data sensitive to brain tissue property changes that precede macroscopic atrophy in the early stages of IPD.

This research aims to determine the brain tissue property changes induced by neurodegeneration that can be linked to clinical phenotypes which will allow us to create a predictive model for early diagnosis in IPD.

We hypothesized that the degree of disease progression in IPD patients will have a differential and specific impact on brain tissue properties used to create a predictive model of motor and non-motor impairment in IPD.

We studied the potential of in-vivo quantitative imaging sensitive to neurodegeneration-related brain tissue characteristics to detect changes in patients with IPD. We carried out methodological work within the well established SPM8 framework to estimate the sensitivity of tissue probability maps for automated tissue classification for detection of early IPD. We performed whole-brain multi parameter mapping at high resolution followed by voxel-based morphometric (VBM) analysis and voxel-based quantification (VBQ) comparing healthy subjects to IPD patients.

We found a trend demonstrating non-significant tissue property changes in the olfactory bulb area using the MT and R1 parameter with $p<0.001$. Comparing to the IPD patients, the healthy group presented a bilateral higher MT and R1 intensity in this specific functional region. These results did not correlate with age, severity or duration of disease. We failed to demonstrate any changes with the R2* parameter.

We interpreted our findings as demyelination of the olfactory tract, which is clinically represented as anosmia. However, the lack of correlation with duration or severity complicates its implications in the creation of a predictive model of impairment in IPD.

KEYWORDS: Idiopathic Parkinson’s disease, Magnetisation transfer (MT), R1, R2*, Quantification.

INTRODUCTION:

Idiopathic Parkinson disease (IPD) is a late-onset movement disorder characterized by the classical triad of tremor, rigidity, and bradykinesia. Movement disorder specialists are able to detect first clinical signs at a more advanced stage of neurodegeneration with 70% loss of dopaminergic neurons affecting the functional integrity of the nigro-striatal pathway.

IPD is also characterised by non-motor deficits. Some of those, like gastrointestinal and urinary dysfunction, cardiovascular problems, anosmia, sleep disorders, depression and pain are the ones to be found in the early state of IPD, even years before the apparition of the motor symptoms. The problem is that these are common and variable signs that can easily go unnoticed because of their high frequency in the healthy population. This underlines the pressing need for an accurate early diagnosis, which will allow neuro-protective treatments to be administered before critical number of neurons is already destroyed.

Parkinson's disease is linked with whole brain changes, in the striatum as well as in the cortex and sub cortex with accumulation of Lewy bodies, alpha-synuclein and neuronal loss. Some invasive neuroimaging studies found that those changes render some regions 'underactive' in akinetic Parkinson, like the supplementary motor area (SMA) (1,2,3,4,5), but some other regions, like the cerebellum, the parietal cortex and the lateral pre-motor cortex, become 'overactive' (3,6,7,8). The Neuropathology of sporadic Parkinson disease early stage that is correlated as stage 2-3 of Braak (9), showed early modifications such as small aggregates of alpha-synuclein with abnormal chemical property, in association with the presence of other altered molecular expression and altered ferritin balance causing iron accumulation, when the small loss of dopaminergic neurons is not enough to be clinical (9).
Even at this stage, the study found biochemical alterations in the frontal cortex (9).

Braak's theory is a classification based on the progression of the Lewy Bodies inclusion following the axon pathway. The biochemical changes first begin in the medulla oblongata and the olfactory bulb at the pre-symptomatic stage 1-2. Then Braak describes stage 3-4, from when the substantia nigra and gray nuclei of the midbrain and forebrain are affected until the pathological changes begin to have clinical meaning correlated with Parkinsonism. Stage 5-6 means the extension of the pathology to the neocortex with major affection of its function (10, 11). Considering that the stage 1-2, with the changes in microstructural properties and the pathological accumulation of Iron, can precede the symptomatic stage from 5 to 10 years, some studies focus on correlating the neuropathology with the neuroimaging.

Neuroimaging provides invasive and non-invasive techniques for characterisation of brain function and tissue properties. Until now, neuroimaging methods have not been very useful for the early diagnosis of IPD especially in patients with short disease duration have only subtle macroscopic signs of neurodegeneration. However, recently, methodological improvements in magnetic resonance imaging have brought techniques allowing novel translational applications of neuroimaging particularly in early diagnosis of neurodegeneration.

Usually, invasive neuroimaging techniques using dopamine tracers such as [18 F]-dopa are used to monitor dopaminergic degeneration in early PD. A study demonstrated, using [18F]-dopa, that << values in the PD patients were lowest, relative to those in the healthy controls, in the posterior putamen contralateral to the side with predominant clinical symptoms>> (12). With progression of symptoms there is loss of dopaminergic projections from the posterior to

the ventral putamen (13). However, we think that it would be not justified to use an invasive technique as a biomarker of early diagnosis for screening purposes in IPD.

Previous research based on magnetic resonance imaging applied region-of-interest (ROI) analysis to demonstrate brain structure changes correlated to the progress of the disease. Volumetric analysis in predefined ROIs showed volume decreases in substantia nigra of patients with IPD (14, 15). However, other brain anatomy parameters mapped with ROI of various sizes demonstrated controversial findings, which can be explained by the arbitrary choice of the ROI. ROI analysis by definition ignores changes in other regions of the brain than the investigated ones (16). A VBM study showed a positive correlation between the degree of olfactory impairment in early IPD and grey matter volume in piriform gyrus and in the amygdala.

Here we aim to find a non-invasive structural MRI biomarker sensitive to changes in tissue characteristics for in-vivo diagnosis in early stages of PD. Advances in computational anatomy methods allow a better automated delineation of substantia nigra and enable the appreciation of the specific tissue properties in a quantitative way.

Computational neuroanatomy using mainly T1-weighted magnetic resonance imaging data provides algorithms for automated brain tissue classification in cerebrospinal fluid (CSF), grey matter (GM) and white matter (WM). The grey-white matter contrast in T1-weighted (T1w) three-dimensional (3D) images allows reliable assessment of cerebral cortex anatomy, but it doesn't reach the same accuracy in sub-cortical structures - caudate, putamen, palladium, substantia nigra and thalamus. The sub-cortical structures are involved in the sensitive-motor functions as well as in the limbic and cognitive system and they play a key role in Idiopathic Parkinson's disease (17).

The first reason for the insufficient grey-white matter contrast in the basal ganglia of T1w images is that these structures have a high concentration of myelinated axons projecting from virtually the entire cortex. These connections represent an intertwined network which, to be delimited, needs a higher spatial resolution than the resolution's limits of T1w, set to about 1mm. This T1w's limit has as side effect, a partial voxel volume averaging in T1w images, with reduced grey-white matter contrast in deep brain structures. The second issue is the high iron content in the basal ganglia GM that shortens the T1w signal, thus reducing the contrast between GM and WM. This leads to a misclassification by the automated segmentation (Here we follow the idea of reference n° 17).

An advanced MRI technique allowing a higher contrast is the magnetization transfer based on an off-resonance radio-frequency stimulus that has a different effect whether the protons are free or whether they are linked to macromolecules. There is a transfer of saturation from linked protons to free protons that we can observe with the Magnetization Transfer Ratio. Since this interaction depends on which macromolecule is linked to the proton, it gives us an indirect inside look of the tissue's physiochemical properties that cannot be generated by classical MRI because the macromolecule pool has too short a transversal relaxation time in order to get their signal captured before losing their coherence. While classical MRI is limited to direct observation of the free proton pool, MT ratio signal is believed to be correlated with the percent of myelin associated lipid in the WM (18).
Being able to have information about the tissue properties brings us to the in-vivo non-invasive structural MRI voxel-based semi-quantitative and quantitative (VBQ) analysis in addition to the VBM analysis.

Other quantitative structural MRI techniques are represented by the relaxation parameters R1 (1/T1) for water, R2* (1/T2) for iron and the water proton density (PD). As it has been said above, so far the brain analysis was limited to morphometric studies with T1w imaging. The volume could be analyzed but T1w is not quantitative. It doesn't give specific tissue property information since T1w maps are constructed based on the relaxation time of T1 (longitudinal relaxation time) and T2 (transversal relaxation time). Each voxel of the T1w imaging sets a mixed contrast, which depends on relative contribution of different tissue content such as myelin, ferritine and water (17).
VBM is used to exhibit the relative morphometric differences as relative volume in regions of interest, generally GM but also WM, with an independent statistical comparison of a voxel-by-voxel analysis of different brains, based on the theory that if a disease occurs it will have macro or mesoscopic variability from a healthy subject (19, 20).

On the other hand, VBQ is more dedicated to analyze the difference in the quantitative MR imaging parameters. It preserves the original quantitative tissue parameters for each voxel so that we can have a look at the microstructural changes that occur before the macroscopic changes in the disease. It is a better way to understand the early stages of Idiopathic Parkinson's disease and to perhaps find a non-invasive in-vivo Parkinson's biomarker. It is possible to have quantitative T1 based images by modulating the intensity of each voxel according to the voxel volume deformation so that the amount of volume tissue is preserved.
VBM and VBQ analysis are set in the Statistical Parametric Mapping (SPM), which processes the data images to allow segmentation (19, 20).

The results of an "Improved segmentation of deep brain grey matter structures using magnetization transfer (MT) parameter maps" (17), were obtained using the SPM5 tools, which use a different a Template a Priori Map (TPM) than SPM8 tools. This is what prompted us to compare the different TPMs.

We are, in the first part of this paper, interest in whether we will obtain the same results with the different TPM's. In the second part we aim to study the potential of in-vivo quantitative imaging sensitive to neurodegeneration-related brain tissue properties to seek for an in-vivo, non-invasive IPD's biomarker.

METHODOLOGY:

Subjects:

We used 18 healthy controls between 30 and 85 years of age (5 male) with a mean age of 54 and 15 patients with IPD (14 medicated patients and one non-medicated) between 51 and 82 years of age (11 male) with a mean age of 62.
The disease duration had a mean of 6.78 years (2 to 13 years, Standard Deviation (SD) 3.57) and the Unified Parkinson's Disease Rating Scale (UPDRS) had a mean of 27.8 (12 to 51, SD 11).

Data acquisition:

All of the data was provided by the LREN Principal Investigator Assistant Professor Bogdan Dranganski.
The 3D datasets were acquired using a 3T whole body MR system with 12-channel RF receive head coil.
A fast acquisition of T1-w anatomical brain imaging was performed based on the 3D modified driven equilibrium Fourier transform (MDEFT) sequence (time repetition TR: 7.92 ms; echoes time TE: 2.48 ms; inversion pulse TI: 910 ms; flip angle: 16°; fat saturation; bandwidth 195 Hz/pixel; acquisition time approximately 13 min; (16, 17)), with an isotropic resolution of 1 mm and compensation for B1 inhomogeneities.

The quantitative MRI protocol for the multi-parameter mapping is based on a 3D multi-echo fast low angle shot (FLASH) that acquired three co-localized datasets with predominant T1-w, MT-w and PD-w (*time repetition (TR)/ flip angle*: T1-w: 18.7 ms/20°, MT-w: 23.7 ms/6°, PD-w: 23.7 ms/6°). Before the acquisition, an off-resonance Gaussian-shaped RF pulse of 4 ms duration, 220° nominal flip angle, 2 kHz frequency offset, was applied (16,17).

We obtained six volumes for each of the three co-localized datasets by capturing the signal of six bipolar gradient echoes. These volumes were then averaged to improve the signal-to-noise-ratio (SNR), resulting in three averaged volumes that were used to calculate the parameter maps (16, 17)
T1-w and PD-w and MT-w averaged volumes were used to calculate T1, the apparent PD (signal amplitude), MT saturation parameter (additional MT saturation percentage created by due to a single MT pulse) and the apparent longitudinal relaxation rate R1 (1/T1) that was corrected for field's inhomogeneities using Unified segmentation based correction UNICORT (16, 17, 19, 20).

Data processing:

We used the SPM8 toolbox that is implemented in the MATLAB (matrix laboratory) software to pre-process the data and analyze it with a VBM and VBQ.
The pre-processing implies intra and inter-subject alignment to correct the effect due to the different positions of the head in the MRI (inter-subject) and the little movements of the subjects during the scanning session (intra-subject), using "rigid-body-transformation" based on a reference image that corresponds to the first image or an average of all the images (16, 17, 19, 20)

We remove the skull from the images by using a PD-w images co-registration with T1-w images and the Data is then segmented into GM (C1), WM (C2), CSF (C3) and three non-brain tissues, before being normalized to the same stereotactic space.

To achieve the segmentation, SPM 8 software uses a combination of a priori probability maps TPM's and the estimation of the intensity distribution of GM and WM (WM has more intensity as GM) based on multiple Gaussians models which allows it to take into account the variance and the means of voxels' intensity as well as the partial volume effect that is created from the signals of the different tissue classes that are contained in one voxel. The Segmentation between GM, WM, and CSF on the SPM software is based on the intensity of the voxels and on a *priori* tissue probability maps (TPMs) that overlay the normalized image

to indicate the probability that a tissue is GM, WM or CSF. The TPMs are implanted in the SPM8, to get more concordance with the brain segmentation, knowing that each brain varies from each other (16, 17, 19, 20).
There were three priors TPMs included in the SPM8 software that we used. The most recent segmentation map is used by default in the SPM8 but there is still the possibility to change to the previous TPMs that were used in SPM5. The TPMs were developed by the International Consortium for Brain Mapping (ICBM) (19, 20, 21).

Dartel (diffeomorphic registration algorithm) is a "non-rigid body" inter-subject alignment to perform the spatial normalization. It involves 6.000.000 coefficients so that after the match of one brain's region it will still have enough freedom to match other regions with good alignment accuracy (19, 20)
The GM and WM tissue classification resulting from the segmentation will be used to generate a template based on the average of all subjects' TPM. Then Dartel wraps simultaneously the TPM's of GM and WM for each subject into a nonlinear alignment with the template, creating a "flow field" for each subject that represents the deformation that was applied during the wrapping process.
The output data is then aligned in the same stereotactic space called MNI space. A Jacobian determinant takes into account the linear (rigid-body) and the non-linear deformation for each voxel to keep the original tissue's volume by modulating proportionally the intensity of the wrapped voxel (19, 20, 22).

Before we access the statistical analysis, the images have to be smoothed with an isotropic Gaussian kernel set to [6 6 6] FWHM. The smoothing screens each voxel to compare it with the voxels around and blurs the images by filtering the voxels that have an inappropriately high difference with the voxels around.

In order to achieve an optimal comparison between T1 and MT images, we used a co-registration of C1 and C2's MT images with C1 C2's T1 images.

Data statistical analysis:

The data analysis was performed with SPM 8 for a VBM, VBQ, semi-quantitative and quantitative analysis.

For the first part, we created a matrix for statistical analysis using a full factorial design with T1 images, MT images, patients (pat) and controls (ctrl) as factors. Total intracranial volume (TIV), age and gender were the co-variants.
We implemented the same design for all three segmentation templates a priori maps TPM (SPM 8 TPM, New grey TPM, and Grey TPM). The analyses were performed both on separates designs matrix for each TPM and on a mass-univariate approach with a single block-diagonal design matrix containing all three TPM.
We used then a t-test looking for difference between the three TPM, T1 and MT, IPD's patients and healthy people.
We applied the threshold at $p < 0.05$ using FEW (family-wise error) to get a significant level.

The results of this part will allow us to confirm that MT is more appropriate for the analysis of the deep structures that are concerned by IPD and it also allows us be critical of the use of the TPM that we will be using for the second part of this research.

The second part of this study is based on the quantitative analyses of MT, R1 and R2* parameters.
We used the previous chosen TPM to process the images and analyzed them with a full factorial design in a single block matrix, using this time R2*, R1, MT intensity parameter, patients and controls as factors and TIV, gender and age as co-variant.
Following, we performed a t-test to look for differences between IPD's patients and healthy.
For an optimal analysis of our results, we added a study of the correlation for each intensity parameter with age, duration of IPD, severity of IPD, severity of IPD with duration, TIV and gender.

We applied two thresholds: first at a non-significant threshold of $p < 0.001$ to detect any trend, and a second threshold at $p < 0.05$ using FWE (family-wise error) to get a significant level.

RESULTS:

Deep brain structure's delimitation with T1 and MT.

The voxel-based-morphometry (VBM, images 1 and 2) indicated a higher contrast between deep brain's structures and WM for the MT maps compared to the MDEFT T1 maps. Substantia nigra, palladium, caudal putamen, dentate nuclei of the cerebellum and other nuclei of the brainstem (periaquaductal grey nuclei, reticular formation) are significantly (FEW with $p<0.05$) better isolated with the segmentation based on the MT maps.

Image1a. : ***T-test using single block matrix design, with all three TPM matrix and T1>MT as contrast.***

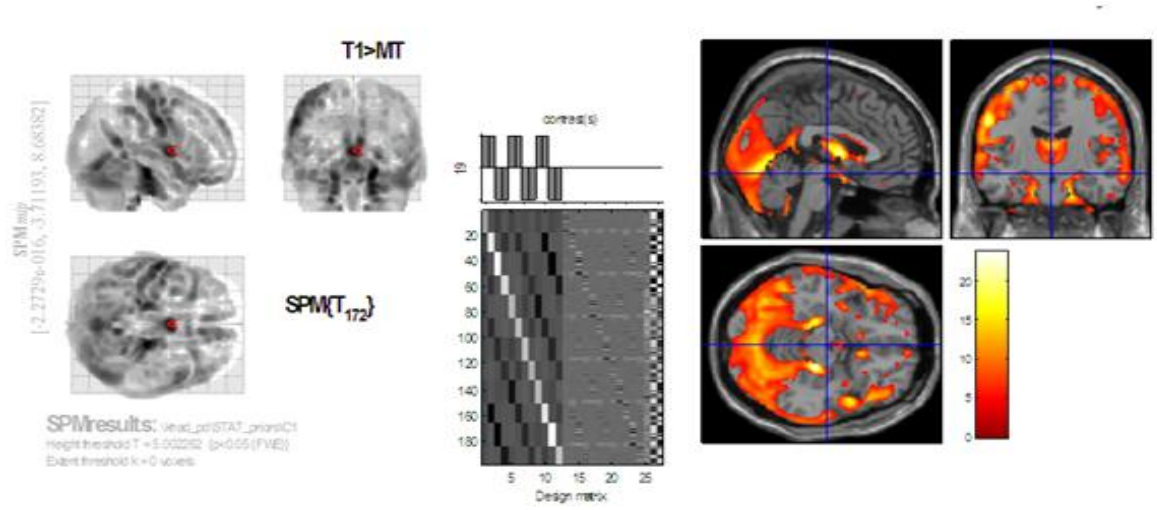

Image1b. : ***T-test using single block matrix design, with all three TPM matrix and T1<MT as contrast.***

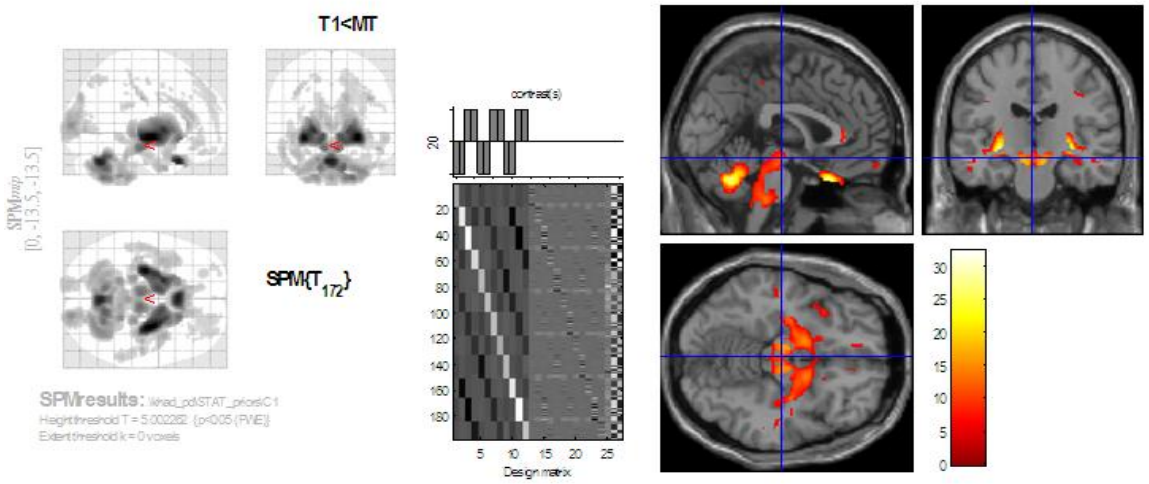

Differences between GM estimation with three various Template priori map's (TPM): SPM8 vs. GreyNew vs. Grey (the last two are from SPM5).

The three different TPM's for GM segmentation are presented in image 2. We can clearly notice that the SPM 8 TPM is sharper than the other two TPM's however we loose substantia nigra isolation on the SPM 8's TPM (cross-section images).

Image 2: ***Templates of priori maps.***

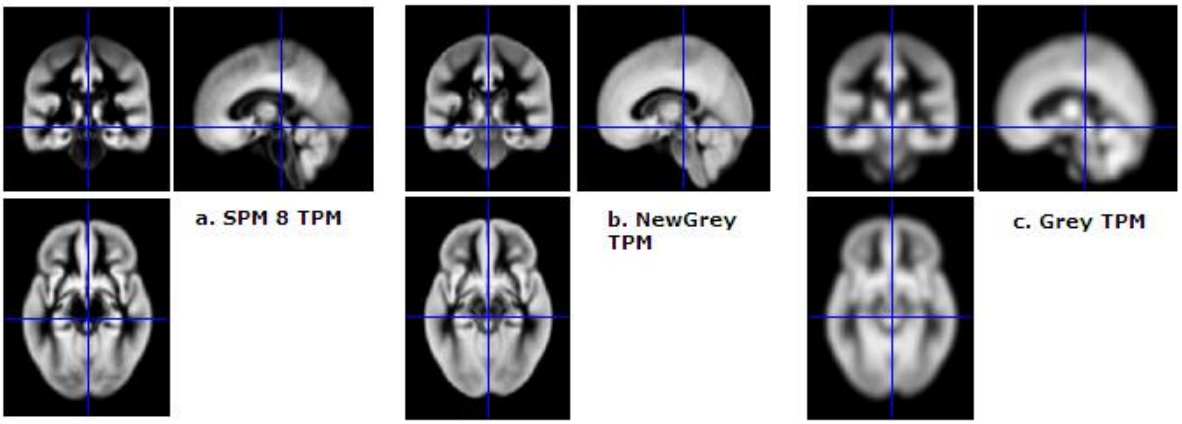

The images below allow a better understanding of the difference between the three templates. Both NewGrey and Grey TPM indicated more volume in the cortex area and in the deep brain structures. There is a visual overestimation of the cortex's GM within the SPM 5 templates (NewGrey and Grey) while SPM8 doesn't allow a good analysis of the deep brain structures of IPD's patient given the substantia nigra is not visible with it.

***Image 3:* T-test with contrasts in favor of SPM8 TPM.**

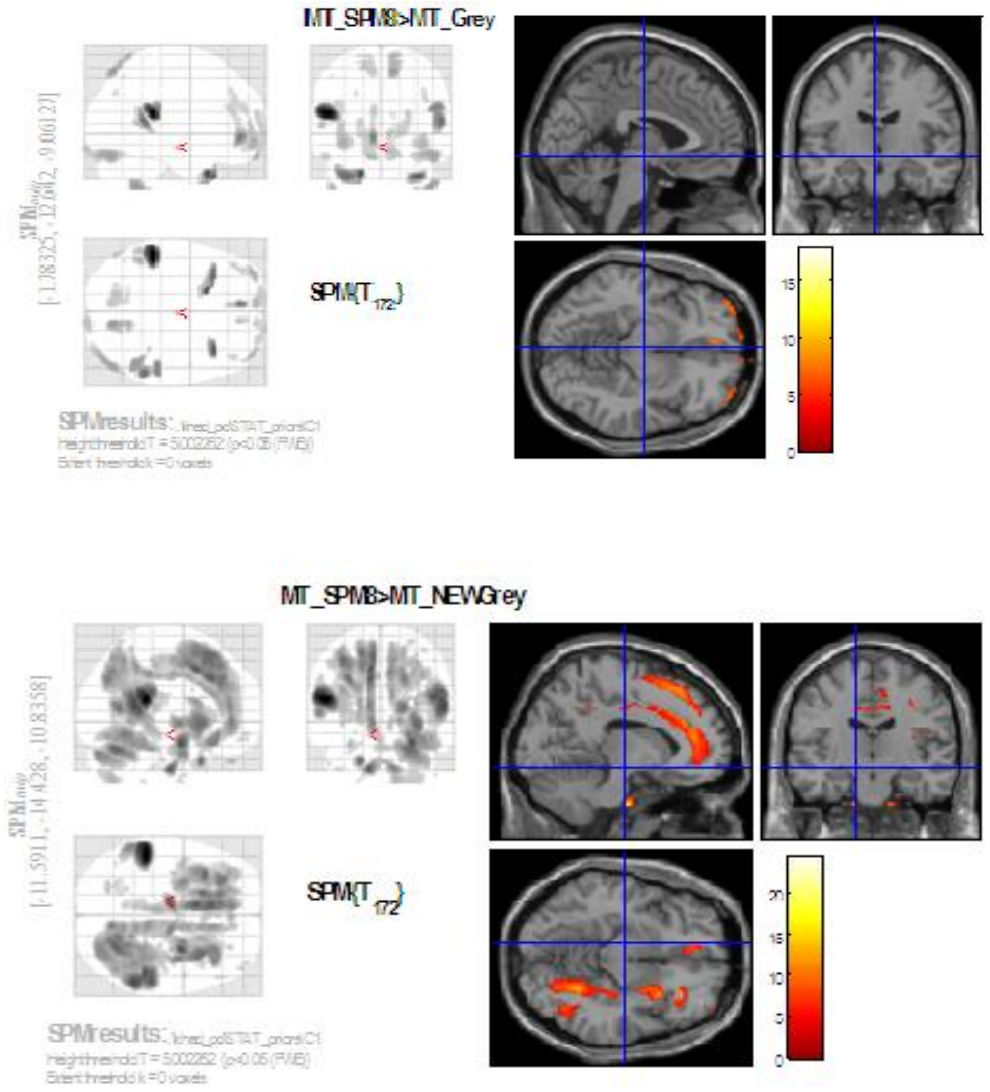

NewGrey TPM is a compromise between the SPM8 TPM and the Grey TPM. The blurriness of the TPM provided a better isolation of substantia nigra, ventral thalamus and putamen. Within image 4, the estimation of the cortex's volume is larger with the NewGrey TPM than SPM8 TPM.

<u>Image 4:</u> T-test with contrast in favor of NewGrey.

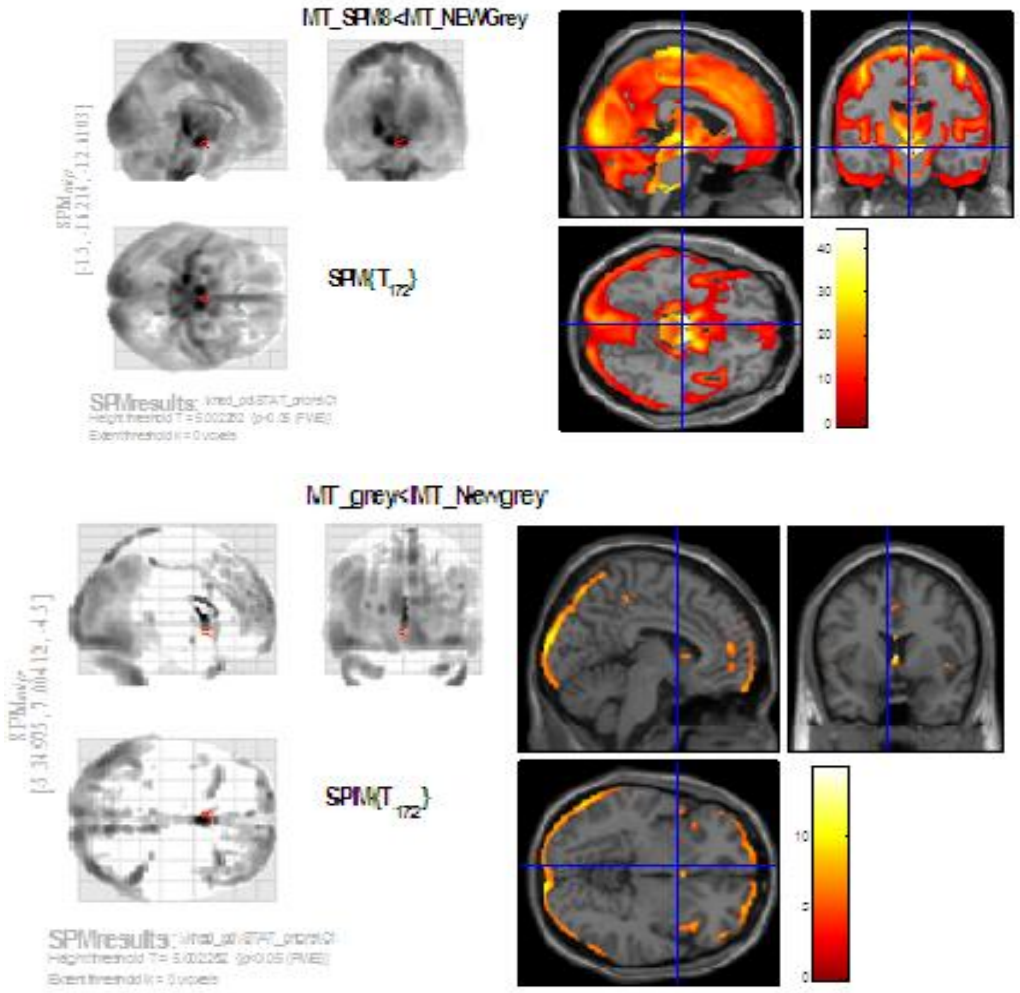

The Grey TPM is the most blurred one (image 5). The higher priori probability of GM for each voxel allows a larger isolation of deep brain structure. Substantia nigra, ventral thalamus, palladium and putamen are all highlighted within the Grey TPM.
Cortex volume segmentation is larger within this TPM than with the other two TPMs.

<u>Image 5:</u> T-test with contrast in favor of Grey TPM.

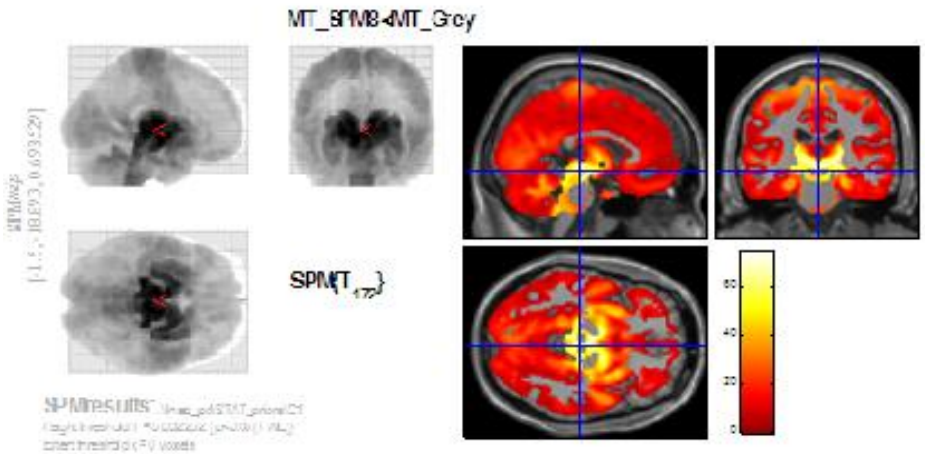

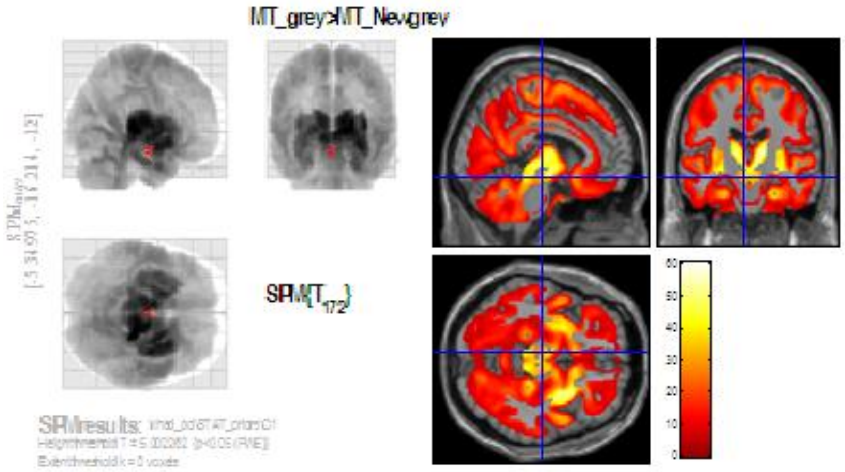

<u>Differences between IPD patients and control group based on VBM analysis.</u>

Images 6 and 7 indicated no significant or relevant volume changes (FEW correction, $p<0.05$) between the controlled group that we scanned and the IPD patients we included in our research.

<u>Image 6:</u> Image obtained with GreyNew TPM analysis, showing that there is no region with a larger volume in the control group to demonstrate degeneration.

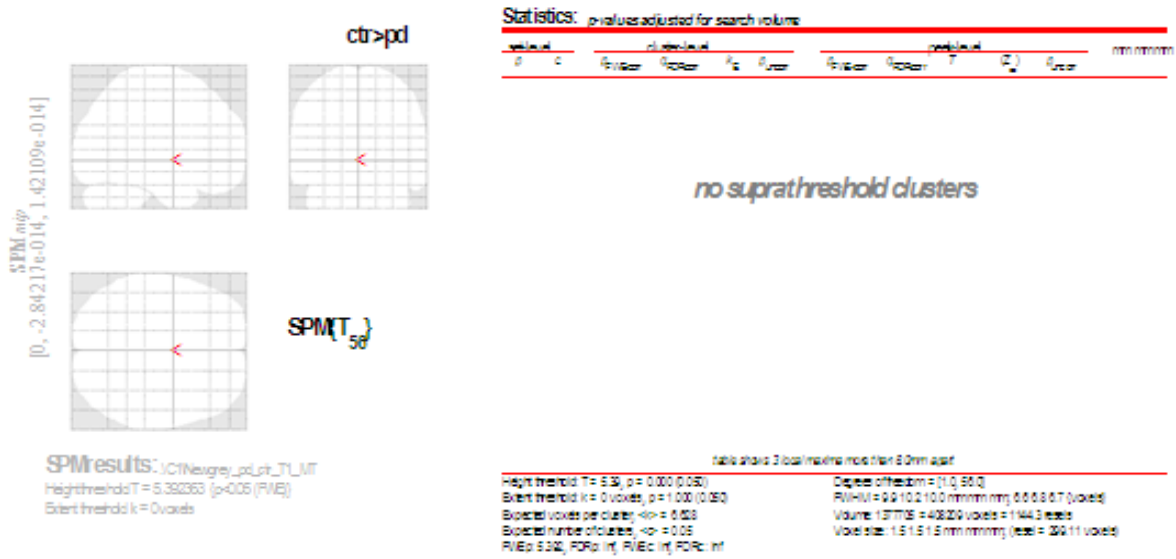

Image 7: ***Image obtained with GreyNew TPM analysis, showing that there is no relevant area with higher volume in the patient group.***

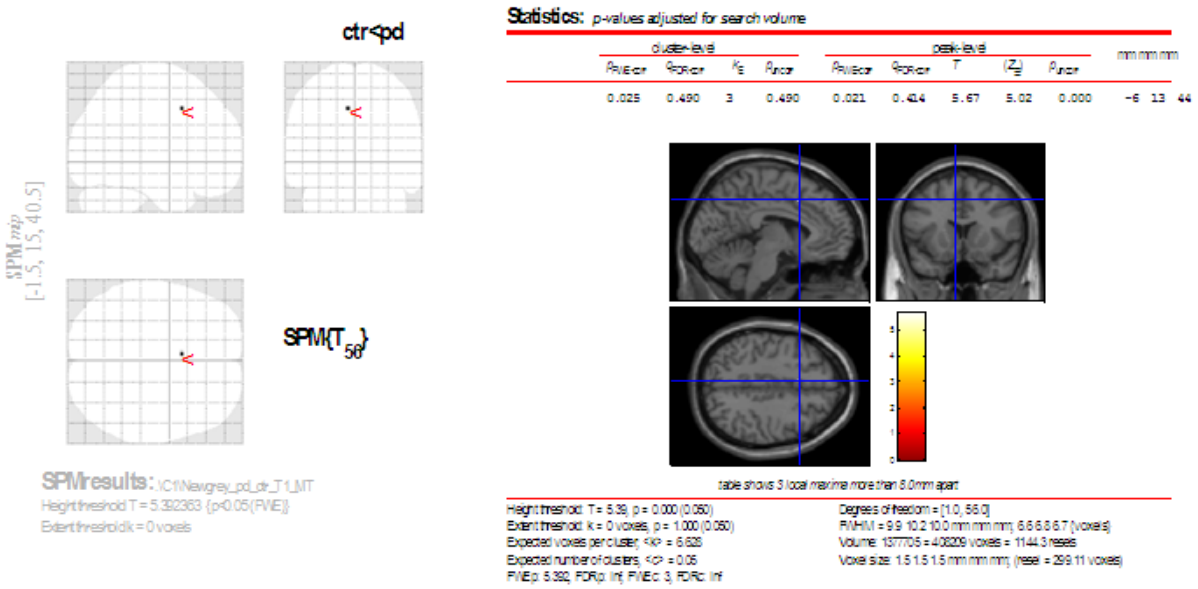

Tissue properties analysis based on R2*, R1 and MT maps intensity.

R2* voxel-based-quantification:

The R2* analysis didn't reveal any specific pattern or functional region with higher intensity in any of the two groups. Analysis with positive and negative correlation to the age, duration and severity also did not produce any specific results.

R1 voxel-based-quantification:

R1 images demonstrate a bilateral higher intensity on the olfactory bulb and tract with the uncorrected threshold set to p<0.001(no FEW, image 8). These results are not connected with a positive correlation to the age. A negative correlation to the age within the R1 analysis tends to demonstrate a global activation of the brain with more intensity for the temporal lobe. The negative correlation to the disease duration shows higher R1 intensity in the premotor, motor and sensitive cortex.

There were no specific regions that correlated with the severity or the severity*duration of the disease.

***Image 8:* R1 parameter showed olfactory bulb higher intensity within controls in comparison with patients with Parkinson's disease.**

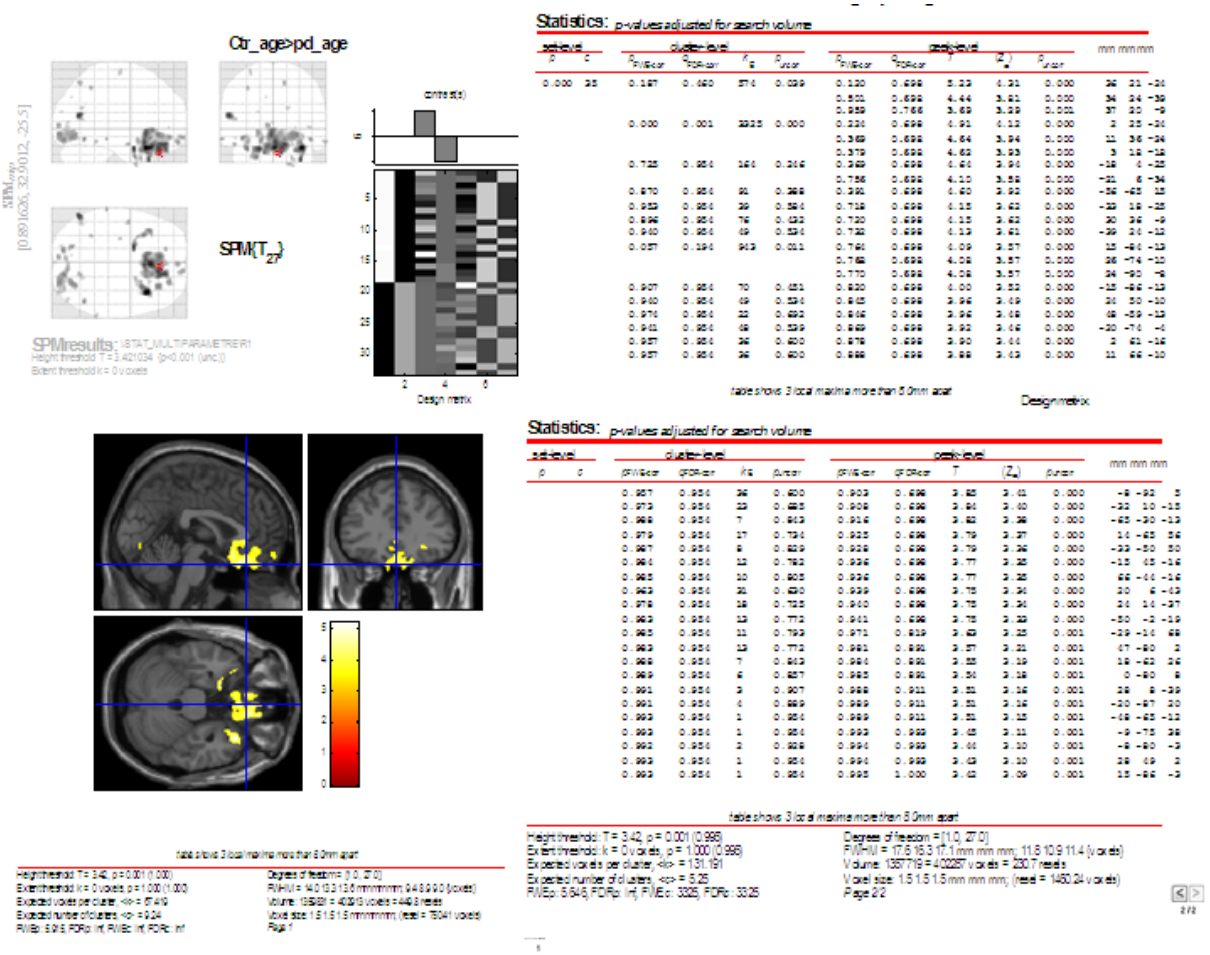

MT voxel-based-quantification:

The control group, in comparison to the patients, revealed a higher MT intensity in the area of the olfactory bulb (image 9). These results were negatively correlated with the age and positively correlated with the severity.

The MT intensity showed a negative correlation with the duration for the pre-motor, motor and sensitive cortex.

There were no specific regions that correlated with the severity*duration.

<u>Image 9:</u> MT parameter showed olfactory bulb higher intensity within the control group in comparison with patients with Parkinson's disease.

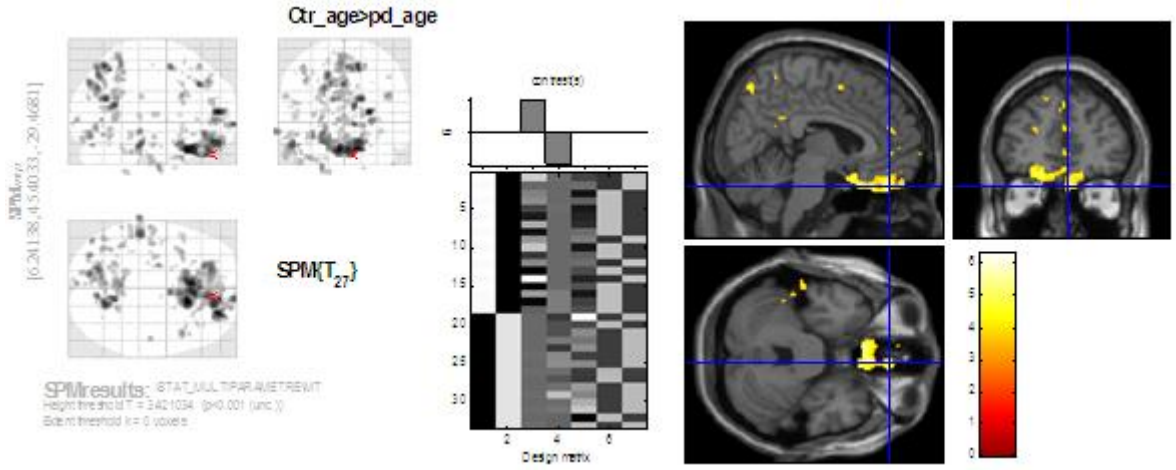

The MT analysis didn't reveal a specific area with more intensity for the patient group compared to the control group.

DISCUSSION:

- The first results demonstrated a significant better delineation of deep brain structures with MT map rather than T1 MDEFT.

-VBM analysis didn't detect any volume changes between IPD patients and the control group.

-VBQ analysis of the three quantitative parameters (R2*, R1 and MT intensity) show a trend towards changes in the olfactory bulb.

We confirmed the results of an "Improved segmentation of deep brain grey matter structures using magnetization transfer (MT) parameter maps" (17). T1 images are influenced by the high iron content of deep brain GM which reduced the T1 relaxation and confused the detection of basal nuclei as GM (WM has a shorter relaxation time as the GM). MT maps allow a better estimation of the myelin's content and therefore of the WM-GM segmentation.

Furthermore we have demonstrated that a blurred TPM raises the priori probability of each voxel to be estimated as GM. Since basal nuclei are rarely segmented because of all their projection (WM) as well as the high content of iron, a blurred template allows more flexibility to detect these structures. The consequence of the blurriness is an overestimation of the cortex. By increasing the TPM's sharpness, SPM 8 affords a more accurate delimitation and analysis of the cortex but it then makes it difficult to analyze the deep brain structures implicated in the IPD.

The Grey TPM, the most blurred one, has clearly highlighted the substantia nigra, the ventral thalamus, and both the palladium and put amen. We decided however not to use this TPM

because of the overestimation of the GM on the cortex. As our research is based on a whole brain analysis, our hypothesis was that the NewGrey TPM is more appropriate given it's a balance between the substantia nigra and the GM overestimation. This was further decided by the fact that even deep brain structures might be overestimated with the Grey TPM.
Note that we did not use the SPM 8 TPM because it didn't present an accurate isolation of the substantia nigra, one of the main regions that degenerated in IPD.

Even if, because of the time restriction, we decided to only apply the GreyNew TPM to search for tissue characteristics with MT, R1 and R2* parameters, it would be more interesting to perform a parametric analysis with the other TPM to have larger view of the statistical consequences of choosing one TPM rather another.

The VBM analysis didn't reveal any significant volume changes. That can be explained by the fact that most of our patients are still in the early stages of IPD where no changes can be seen on the MR images. We also performed the statistics with a FWE correction based on a whole brain analysis which reduces the probability to detect voxels with different volumes in the IPD group compared to the control group. It would have been possible to do a Region of interest analysis to raise the probability of detecting changes in the basal ganglia but research that demonstrates substantia nigra degeneration (14, 15) already exists and therefore we decided to concentrate on the global view of IPD with a whole brain analysis without limitation to any specific region.

Quantitative results:

R2* images with the VBQ analysis didn't give any significant results, even when the other studies succeed to demonstrate a significant higher R2* intensity within the substantia nigra of the patient with Parkinson's disease (15, 23). R2* intensity increases with the accumulation of iron content provoked by the degeneration.
The little number of patient with IPD (n=15), the early stage in the disease (UPDRS mean 27.8) and the fact that all the IPD patient's, except one of them (UPDRS 20), are on medication delaying the progress of degeneration might explain our failure to demonstrate any differences. We set the hypothesis that our patient group yet doesn't have a visual MRI degeneration in substantia nigra.

The other VBQ parameters, R1 and MT revealed a bilateral higher intensity located on the olfactory bulb area of the control group compared to the IPD patient.
MT images are strongly correlated with myelin content (18, 24). R1 intensity increases with myelinisation since it's correlated with the extracellular water content trapped between the myelin's layers. This explains why MT and R1 images are correlated up to 90%.
The results are not clearly significant but are relevant with the consistency of MT and R1. As we know, one of the early sign of IPD is anosmia, and we succeed to demonstrate a trend of myelin's reduction in the olfactory bulb area with in-vivo non-invasive neuroimaging parameters. Those results do not correlate with age, severity or duration of the disease. The fact that the results are not correlated with age, underline IPD as the main cause of loss of myelin. However, the lack of correlation with the severity or duration makes it difficult to create a predictive model for early detection of Parkinson based on a linear interaction between MRI founding and clinical assessment.
The uncorrelated results in the olfactory bulb are presumably due to the early occurrence of anosmia in IPD. In our IPD patients group the atrophy of the olfactory tracts are probably too

advanced. In order to find a correlation we should restrict patients with Braak's stage 1for this research however, the patients in Braak's stage 1 cannot be clinically diagnosed.

Methodological considerations:

The quantitative data acquisition was performed by Professor Bogdan Draganski with a high-resolution multi-parameter mapping based on a 3D multi-echo FLASH.
The control of systemic errors was performed with statistical methods for corrections of radiofrequency (RF) transmit inhomogeneities using UNICORT and DARTEL.

One of the main limitations was the lack of precision in the assessment of clinical phenotype of the patients. We knew the UPDRS scores, but we didn't know which features were deficient. To create a predictive model for early diagnosis in IPD it would be interesting to have several IPD groups with the same IPD stage within one group, but with different stages between the different groups.
Another possibility would be to proceed with a cohort of random people looking for quantitative MT and R1 changes in the olfactory bulb and following them in time to determinate which percentage will develop IPD.

The other main limitation was the time restriction to perform this study. It would have been interesting to perform a multi-parameter analyses combining MT, R1 and R2* instead of only analyzing them separately.

Conclusion:

In conclusion we managed to demonstrate an in-vivo pathophysiological process of IPD neurodegeneration with a non-invasive MRI technique using tissue characteristics' changes.
Our results didn't allow the creation of a predictive model for early IPD, but it shows the potential of quantitative imaging.

Acknowledgements:

We acknowledge the support of the LREN's team (Laboratoire de recherche en neuroimagerie), which is part of the Department of Clinical Neurosciences (UNIL/CHUV).

BIBLIOGRAPHIE:

1. Playford ED, Jenkins IH, Passingham RE, Nutt J, Frackowiak RS, Brooks DJ. Impaired mesial frontal and putamen activation in Parkinson's disease: a positron emission tomography study. Ann Neurol. 1992 Aug; 32(2):151-61.
2. Rascol O, Sabatini U, Chollet F, Celsis P, Montastruc JL, Marc-Vergnes JP, et al. Supplementary and primary sensory motor area activity in Parkinson's disease. Regional cerebral blood flow changes during finger movements and effects of apomorphine. Arch Neurol. 1992 Feb; 49(2):144-8
3. Sabatini U, Boulanouar K, Fabre N, Martin F, Carel C, Colonnese C, et al. Cortical motor reorganization in akinetic patients with Parkinson's disease: a functional MRI study. Brain. 2000 Feb; 123 (Pt 2):394-403.
4. Jahanshahi M, Jenkins IH , Brown RG Marsden CD, Passingham RE, Brooks DJ, et al. Self-initiated versus externally triggered movements: I. An investigation using measurement of regional cerebral blood flow with PET and movement-related potentials in normal and Parkinson's disease subjects. Brain 1995, volume 118, Issue 4 Pp. 913-933.
5. Patrice Péran, Andrea Cherubini, Francesca Assogna, Fabrizio Piras, Carlo Quattrocchi, Antonella Peppe, et al. Magnetic resonance imaging markers of Parkinson's disease nigrostriatal signature. Brain 2010: 133, Issue 11, Pp. 3423-3433.
6. Rascol O, Sabatini U, Fabre N, Brefel C, Loubinoux I, Celsis P, et al. The ipsilateral cerebellar hemisphere is overactive during hand movements in akinetic parkinsonian patients. Brain 1997; 120: 103-110.
7. Samuel M, Ceballos-Baumann AO, Blin J, Uema T, Boecker H, Passingham RE, et al. Evidence for lateral premotor and parietal overactivity in Parkinson's disease during sequential and bimanual movements. A PET study. Brain 199/, volume 120, issue 6: 963-976.
8. Yu H, Sternad D, Corcos DM, Vaillantcourt DE. Role of Hyperactive Cerebellum and Motor Cortex in Parkinson's Disease. Neuroimage. 2007 March; 35(1): 222–233. Available: http://www. ncbi.nlm.nih.gov/pmc/articles/PMC1853309/
9. Ferrer I, Martinez A, Blanco R, Dalfó, Carmona M. Neuropathology of sporadic Parkinson disease before the appearance of parkinsonism: preclinical Parkinson disease. Journal of Neural Transmission, May 2011, Volume 118, Issue 5, pp 821-839.
10. Braak H, Ghebremedhin E, Rüb U, Bratzke H, Del Tredici K. Stages in the development of Parkinson's disease-related pathology. Cell Tissue Res. 2004 Oct; 318(1):121-34.
11. Braak H, Tredici KD, Rüb U, de Vos RAI, Jansen Steur ENH, Braak E. Staging of brain pathology related to sporadic Parkinson's disease**.** Neurobiology of AgingVolume 24, Issue 2, March–April 2003, Pages 197–211.
12. Jokinen P, Helenius H, Rauhala E, Brück A, Eskola O, Rinne JO. Simple ratio analysis of 18F-fluorodopa uptake in striatal subregions separates patients with early Parkinson disease from healthy controls. J Nucl Med. 2009 Jun; 50(6):893-9.
    Availble: http://jnm.snmjournals.org/content/50/6/893.long
13. P. K. Morrish, G. V. Sawle, D. J. Brooks. Regional changes in [^{18}F]dopa metabolism in the striatum in Parkinson's disease. Brain 1996, Volume 119, Issue 6, Pp. 2097-2103.
14. Draganski B, Bhatia KP. Brain structure in movement disorders: a neuroimaging perspective. Current Opinion in Neurology: August 2010 - Volume 23 - Issue 4 - p 413–419
15. Menke RA, Scholz J, Miller KL, Deoni S, Jbabdi S, Matthews PM et al. MRI characteristics of the substantia nigra in Parkinson's disease: a combined quantitative T1 and DTI study. Neuroimage. 2009 Aug 15; 47(2):435-41.
16. Draganski B, Ashburner J, Hutton C, Kherif F, Frackowiak RS, Helms G et al. Regional specificity of MRI contrast parameter changes in normal ageing revealed by voxel-based quantification (VBQ). Neuroimage. 2011 Apr 15; 55(4):1423-34.
17. G. Helms, B. Draganski, R. Frackowiak, J. Ashburner, and N. Weiskopf. Improved segmentation of deep brain grey matter structures using magnetization transfer (MT) parameter maps. NeuroImage 2009, 47(1):194-198.

18. Tofts PS, Steens SCA, van Buchem MA. Quantitative MRI of the Brain: Measuring Changes Caused by Disease. Chapter 8: MT: magnetization transfer. In: Tofts PS, editor. Chichester: John Wiley & Sons Ltd; 2003. pp. 257–298.
19. Ashburner J. Computational anatomy with the SPM software. Magnetic Resonance Imaging, volume 27, Issue 8, October 2009, Pages 1163–1174.
20. Mechelli A, Price CJ, Friston KJ, Ashburner J. Voxel-Based Morphometry of the Human Brain: Methods and Applications. Current Medical Imaging Reviews, Volume 1, Number 2, June 2005, pp. 105-113(9).
Available: http://www.fil.ion.ucl.ac.uk/spm/doc/papers/am_vbmreview.pdf
21. Mazziotta J, Toga A, Evans A, Fox P, Lancaster J, Zilles K, et al. A probabilistic atlas and reference system for the human brain: International Consortium for Brain Mapping (ICBM). Philosophical Transactions of the Royal Society B; Biological Science, 29 August 2001, vol. 356 no. 1412 1293-1322
22. Ashburner J. and Friston K.J. Unified segmentation. NeuroImage 26 (2005) 839 – 851
23. W. R. Wayne Martin, Wieler M, and Gee M. Midbrain iron content in early Parkinson disease: A potential biomarker of disease status. Neurology (2008) Volume: 70, Issue: 16 Pt 2, Pages: 1411-1417
24. Samsonov A, Alexander AL, Pouria Mossahebi, Wu Y-C, Duncan ID, Field AS. Quantitative MR imaging of two-pool magnetization transfer model parameters in myelin mutant shaking pup.